

# Unidirectional magneto-optic polarization converters

M. Lohmeyer\*, N. Bahlmann, O. Zhuromskyy, H. Dötsch, P. Hertel

Department of Physics, University of Osnabrück,

Barbarastraße 7, D-49069 Osnabrück, Germany

---

**Abstract:** Inclination of the bias magnetization in a magneto-optic waveguide yields both non-reciprocal phase shifts and polarization conversion. This enables the design of unidirectional polarization converters, i.e. waveguides that switch between orthogonal polarizations for one direction of light propagation, but keep the polarization state for light propagating in the opposite direction. Simulations of double layer raised strip waveguides show that these constraints can be met with properly adjusted geometries. The results lead to the proposal of a polarization independent integrated optical circulator based on two unidirectional polarization converters between a front and a back polarization splitter.

**Keywords:** integrated optics, magneto-optic waveguides, numerical modeling, Faraday effect, optical isolators, optical circulators

**PACS codes:** 42.82.-m 42.82.Et 85.70.Sq 78.20.Ls

---

## 1 Introduction

The traditional optical isolator setup [1] consists of a nonreciprocal Faraday rotator of proper length between two polarizers. These are adjusted at an angle of  $45^\circ$  such that light passes the device in the direction of transmission with the polarization state rotated by  $45^\circ$ . At the same time, oppositely propagating light is blocked. Due to the need of a  $45^\circ$  polarizer, a direct integrated optical realization of this concept is difficult. While success with a hybrid setup has been reported e.g. in Ref. [2], a monolithically integrated device would have to be designed with polarization splitters which discriminate modes of different polarization, rather than with arbitrarily orientable polarizers. Input and output are to be restricted to the TE and TM states. This may be achieved with an additional reciprocal polarization converting element, i.e. an optical active or proper anisotropic waveguide, as proposed and realized for microoptic devices [3]. Integration of the probably totally different materials (e.g. quartz) into the garnet basis must be suspected to raise problems. However, in contrast to the bulk configuration, for waveguide based devices there is a way to achieve the exact effect of a  $45^\circ$  Faraday rotator in line with a  $45^\circ$  optical active element *without* the latter.

For longitudinally magnetized gyrotropic waveguides employed as polarization converters, the phase matching condition is known to be highly sensitive. A small difference in the relevant propagation constants is sufficient to diminish the achievable polarization conversion considerably. We will introduce an additional nonreciprocal phase shift to adjust phase matching for one direction of propagation only. With proper length, the waveguide completely converts TE polarized light to TM polarization. Between two polarization splitters which are transparent for TE light, the device blocks power transmission in the backward direction. In contrast, oppositely propagating TE input light is converted incompletely, with the remaining TE fraction passing the device in the forward direction. As shown in Section 2, it is possible to design an ideally performing isolator which transmits the entire forward input.

This principle of unidirectional polarization conversion has been proposed in Ref. [4], where the authors considered a planar configuration with metal overlays acting as mode selectors. Phase matching between the planar TE and TM modes was achieved by an additional anisotropic superstrate layer. In this paper we investigate raised strip waveguides with two dimensional light confinement where the phase matching conditions may be satisfied by proper choice of the waveguide dimensions [5]. The simulations rely on numerical approximants for the two hybrid fundamental modes, with the magneto-optic effects considered in the framework of coupled

---

\*Fachbereich Physik, Universität Osnabrück  
Tel.: +541/969-2641 Fax: +541/969-2670

Barbarastraße 7, D 49069 Osnabrück  
e-mail: manfred.lohmeyer@physik.uni-osnabrueck.de

mode theory. Double layer films with opposite specific Faraday rotation [6] allow for a considerably reduced device length compared to the planar design, as we shall see.

Similar concepts have been experimentally demonstrated in Refs. [7, 8]. These rely on unidirectional mode conversion between the fundamental TM mode and the first order TE mode [7] or between the  $TM_0$  mode and the set of TE polarized radiation modes [8], caused by a magnetization in equatorial orientation. While both concepts may be less critical with respect to fabrication tolerances due to wide, slightly etched waveguides, they pose problems with respect to integration, since one has to deal either with multimode waveguides or with radiated power. The concepts are not suitable for the realization of circulator devices.

Protection of an optical circuit from backscattered light is the most prominent application of optical isolators. In general, the attached optical network does not preserve polarization, hence arbitrarily polarized reflected light must be blocked. For a light source that is restricted to a single polarization, combination of a single polarization isolator and a properly adjusted polarizer or polarization splitter yields the desired protection. If, in contrast, the circuit's output is not of a specific polarization, e.g. because part of it is constructed by pieces of circular optical fiber, the task requires an isolator with polarization independent performance.

In an integrated optical setting, we thus have to demand proper isolation for both TE and TM input light. The straightforward way to achieve this is to line up a TE and a TM isolator, provided that each device is transparent for the other polarization (note that this is a critical additional constraint for most single polarization concepts). The conventional polarization rotator setup cannot be used, since it involves polarizers.

Alternatively, one may think of one isolator for TE light and one for TM light in parallel, connected to single input and output waveguides by two polarization splitters. Both have to be manufactured side by side on the same substrate, requiring different materials and perhaps perpendicularly directed outer bias fields in close proximity. Similar difficulties arise with the first concept for a non-composite integrated polarization independent isolator, as proposed recently in Ref. [9].

As another alternative, it is tempting to employ the unidirectional polarization converters of Section 2. Almost square magneto-optic double layer waveguide segments [6] are placed between two polarization splitters where we can use the radiatively coupled waveguide design of Ref. [10]. This idea is developed in the second part of this paper.

## 2 Unidirectional polarization converters

We refer to the phase matched raised strip waveguides investigated in Ref. [5], this time etched from a composite magneto-optic film, where the Faraday rotations in the two layers have opposite signs. Figure 1 illustrates the geometry.

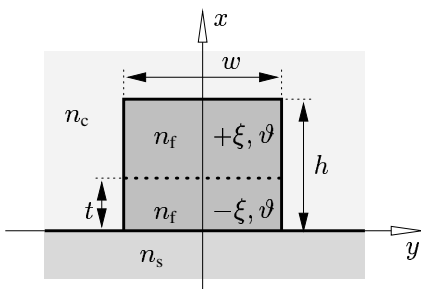


Figure 1: *Magneto-optic double layer waveguide.*  $x$  and  $y$  denote the cross section coordinate axes, light propagates along the  $z$  direction. The strip of height  $h$  and width  $w$  consists of two magneto-optic layers with opposite Faraday rotation ( $\Theta_F \sim \xi$ ). The magnetization is oriented at an angle  $\vartheta$  with respect to the  $z$ -direction in the  $y$ - $z$ -plane.  $t$  denotes the thickness of the bottom layer,  $n_s$ ,  $n_f$ ,  $n_c$  are the refractive indices of the substrate, the guiding film, and the cover, respectively.

For numerical modeling in the framework of coupled mode theory, we split the permittivity tensor in the core region of the waveguide  $\epsilon_f = n_f^2 + \delta\epsilon$  into the contribution of an isotropic refractive index  $n_f$  and a residual

$$\delta\epsilon = i\xi \begin{pmatrix} 0 & \cos \vartheta & -\sin \vartheta \\ -\cos \vartheta & 0 & 0 \\ \sin \vartheta & 0 & 0 \end{pmatrix}, \quad (1)$$

which accounts for the first order magneto-optic effect. The magnetization shall be adjusted in the  $y$ - $z$ -plane, at an angle  $\vartheta$  with respect to the  $z$ -axis.  $\xi$  is related to the specific Faraday-rotation  $\Theta_F$  of the core material by

$\xi = n_f \lambda \Theta_F / \pi$ . This magneto-optic profile yields both nonreciprocal phase shifts, mainly for TM modes, and polarization conversion.

The guided electric and magnetic fields are assumed to be superpositions

$$\mathcal{E}(x, y, z, t) = \sum_j C_j(z) \frac{1}{\sqrt{P_j}} \mathbf{E}_j(x, y) e^{i\omega t}, \quad \mathcal{H}(x, y, z, t) = \sum_j C_j(z) \frac{1}{\sqrt{P_j}} \mathbf{H}_j(x, y) e^{i\omega t}, \quad (2)$$

of the hybrid modes  $\mathbf{E}_j = (E_{jx}, E_{jy}, iE_{jz})$ ,  $\mathbf{H}_j = (H_{jx}, H_{jy}, iH_{jz})$  corresponding to the isotropic structure, normalized by  $P_j = \iint (E_{jx}H_{jy} - E_{jy}H_{jx}) dx dy / 2$ . All of the real valued components  $E_{jx}, \dots, H_{jz}$  are present. The amplitudes  $C_j$  include the harmonic dependence  $\sim \exp(-i\beta_j z)$  on the propagation distance, where  $\beta_j$  denote the propagation constants at a frequency  $\omega$  corresponding to the vacuum wavelength  $\lambda$  and wavenumber  $k = 2\pi/\lambda = \omega\sqrt{\epsilon_0\mu_0}$  for vacuum permittivity  $\epsilon_0$  and permeability  $\mu_0$ .

The unperturbed modes and propagation constants are numerically generated by the fully vectorial mode solver of Ref. [11]. Only the two fundamental modes are relevant. According to their dominant field components, these are specified by indices  $j = \text{TE, TM}$ .

Coupled mode theory as formulated in Ref. [5] predicts TE/TM coupling coefficients

$$\kappa = i \cos \vartheta \frac{\omega \epsilon_0}{4\sqrt{P_{\text{TE}}P_{\text{TM}}}} \iint \xi (E_{\text{TE},x} E_{\text{TM},y} - E_{\text{TE},y} E_{\text{TM},x}) dx dy \quad (3)$$

and magneto-optic phase shifts

$$\delta\beta_j = \sin \vartheta \frac{\omega \epsilon_0}{2P_j} \iint \xi E_{jx} E_{jz} dx dy, \quad j = \text{TE, TM}. \quad (4)$$

As we have found in Ref. [5], the phase shifts remain negligibly small for single layer waveguides. In contrast, for the double layer structures, the maximum TM phase shift, achievable in the equatorial configuration ( $\vartheta = \pi/2$ ), and the TE/TM coupling coefficient in the longitudinal configuration ( $\vartheta = 0$ ) are of equal order of magnitude. This allows the balance of both effects. Figure 2 shows corresponding plots for the coupling coefficient  $\kappa$  and the larger one  $\delta\beta_{\text{TM}}$  of the phase shifts.

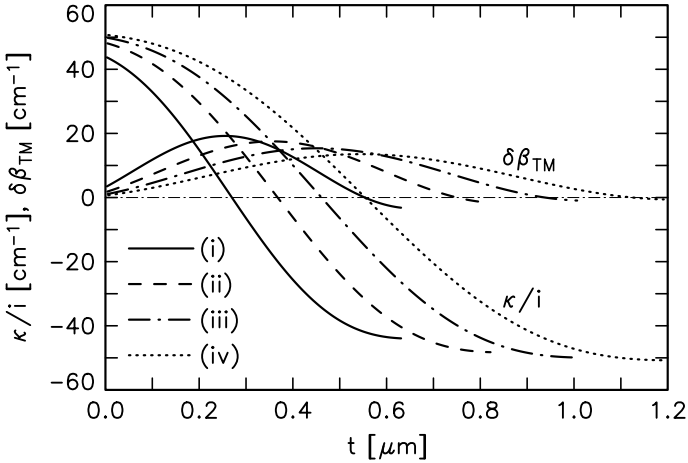


Figure 2: Maximum TE/TM coupling coefficient  $\kappa$  ( $\vartheta = 0$ ) and maximum TM phase shift ( $\vartheta = \pi/2$ ) for double layer waveguides, as sketched in Figure 1, versus the bottom layer thickness  $t$ . (i) to (iv) denote the waveguides of Table 1.

The TM phase shift is approximately proportional to the mode intensity at the central boundary between the magneto-optic layers. This explains the shape of the curves for  $\delta\beta_{\text{TM}}$ . With growing thickness  $t$ , the coupling coefficient  $\kappa$  changes from the maximum value, for a totally positively rotating waveguide, to zero, where the contributions from the bottom and the top layer compensate, and back to the maximum absolute value, for a totally negatively rotating waveguide.

A power transfer ratio  $\eta$  characterizes the polarization conversion. Starting at  $z = 0$  with all power concentrated in the TE mode ( $C_{\text{TM}}(0) = 0$ ), after a distance  $z$  the relative power  $\eta(z) = |C_{\text{TM}}(z)/C_{\text{TE}}(0)|^2$  carried by the TM mode is

$$\eta(z) = \eta_{\text{max}} \sin^2(\rho z) \quad \text{with} \quad \eta_{\text{max}} = \frac{|\kappa|^2}{\rho^2} \quad \text{and} \quad \rho = \sqrt{(\Delta\beta/2)^2 + |\kappa|^2}, \quad (5)$$

where  $\Delta\beta$  is the difference between the shifted propagation constants. The power transfer ratio reaches its maximum  $\eta_{\max}$  at the position of the conversion length  $L_c = \pi/(2\rho)$ .

Reversion of the direction of light propagation can be modeled by inverting the sign of  $\xi$ . While the absolute value of the coupling coefficient  $|\kappa|$  remains unchanged, this operation causes different propagation constants, or phase mismatch values  $\Delta\beta^b = (\beta_{\text{TE}} + \delta\beta_{\text{TE}}) - (\beta_{\text{TM}} + \delta\beta_{\text{TM}})$ ,  $\Delta\beta^f = (\beta_{\text{TE}} - \delta\beta_{\text{TE}}) - (\beta_{\text{TM}} - \delta\beta_{\text{TM}})$  and consequently different conversion lengths  $L_c^f$ ,  $L_c^b$  for forward and backward propagation, respectively.

The final device will have geometry parameters very close to the dimensions of a phase matched waveguide. The magneto-optic profile, determined by the bottom layer thickness  $t$  and by the magnetization angle  $\vartheta$ , is to be adjusted such that the backward phase mismatch vanishes,  $\Delta\beta^b = 0$ . This constraint enables complete polarization conversion,  $\eta_{\max}^b = 1$ , in the backward direction and fixes the device length to one backward conversion length  $L_c^b$ . The resulting mismatch for forward propagating light is  $\Delta\beta^f = 2(\delta\beta_{\text{TM}} - \delta\beta_{\text{TE}})$ . Besides a reduction of the maximum conversion, the additional phase mismatch leads to a shorter conversion length  $L_c^f$ . The forward conversion does not reach pure TM polarization,  $\eta_{\max}^f < 1$ , but after propagating over a distance of an even multiple of  $L_c^f$ , the light is purely TE polarized again. Thus for optimal isolator performance all parameters have to be adjusted such that

$$L_c^b = \frac{\pi}{2|\kappa|} = 2mL_c^f = \frac{m\pi}{\sqrt{(\Delta\beta^f/2)^2 + |\kappa|^2}} \quad (6)$$

holds, with a natural number  $m$ . Increasing the phase mismatch  $|\Delta\beta^f|/2 \approx |\delta\beta_{\text{TM}}|$  by adjustment of  $t$  implies reduction of  $|\kappa|$ , or lengthening the device, respectively (cf. Figure 2). Therefore,  $m = 1$  is the proper choice for Eq. (6). This amounts to a condition for ideal isolation and loss

$$|\kappa| = \frac{1}{2\sqrt{3}} |\Delta\beta^f| \quad \text{or} \quad |\kappa| = \frac{1}{\sqrt{3}} |\delta\beta_{\text{TM}} - \delta\beta_{\text{TE}}|, \quad (7)$$

in addition to the constraint of backward phase matching  $\Delta\beta^b = 0$ .

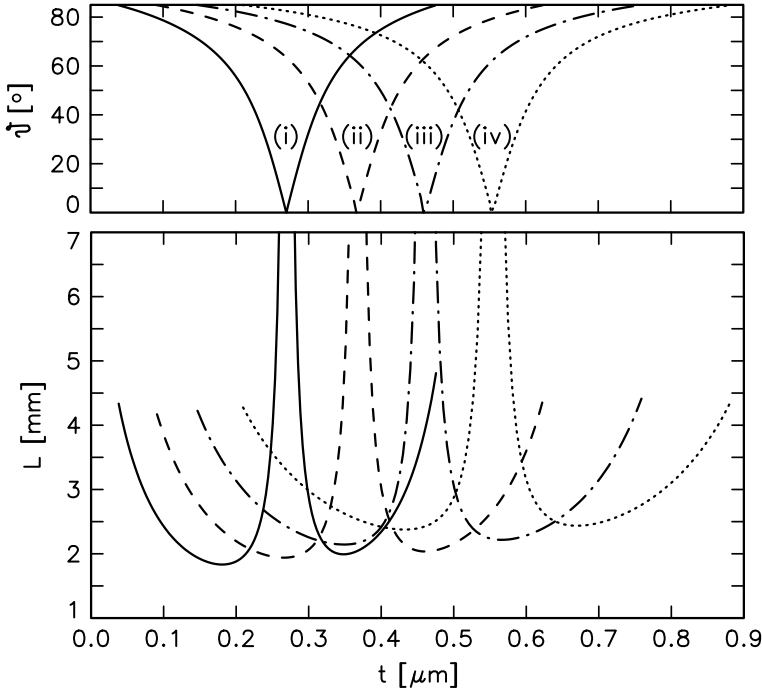


Figure 3: Optimum angle for isolator performance  $\vartheta$  (top) and resulting isolator device length  $L$  versus the thickness  $t$  of the lower layer (bottom), for phase shifting and polarization converting waveguides as sketched in Figure 1, with parameters of Table 1.

According to Figure 3, the condition (7) can be met for most configurations  $t$  with a properly selected angle  $\vartheta$  of the magnetization. The lower part of the figure shows the resulting optimum device length  $L = L_c^b = \pi/(2|\kappa|)$ . Aiming at short devices, the magneto-optic profile should be adjusted to the parameters given by the minima of these curves. Table 1 summarizes parameters for backward phase matched, polarization converting and phase shifting isolator waveguides.

	(i)	(ii)	(iii)	(iv)
$h/\mu\text{m}$	0.634	0.826	1.012	1.198
$w/\mu\text{m}$	0.798	0.995	1.191	1.387
$t/\mu\text{m}$	0.181	0.264	0.349	0.431
$\vartheta/^\circ$	63	65	66	68
$L/\text{mm}$	1.83	1.94	2.14	2.38

Table 1: Parameters for isolating waveguides, according to Figure 1. The remaining quantities are  $n_s = 1.95$ ,  $n_f = 2.302$ ,  $n_c = 1.0$ ,  $\lambda = 1.3\ \mu\text{m}$ ,  $\xi = \pm 0.005$ , corresponding to  $\Theta_F = \pm 3000^\circ/\text{cm}$ .

In contrast to the  $45^\circ$  polarization converters investigated in Ref. [5], only part of the magneto-optic effect is available for polarization conversion, and the device length must match a complete conversion length, instead of its half. Therefore the waveguides are to be about six times as long as those for the conventional setup. While a total length of 2 mm is still tolerable, one has to deal with tolerances which are about six times as strict as those given in our former investigation [5] (cf. this reference for more details about the tolerances). This price has to be paid for the change of input and output from TE/ $45^\circ$  polarized light to TE and TM modes, and the possibility of monolithic integration.

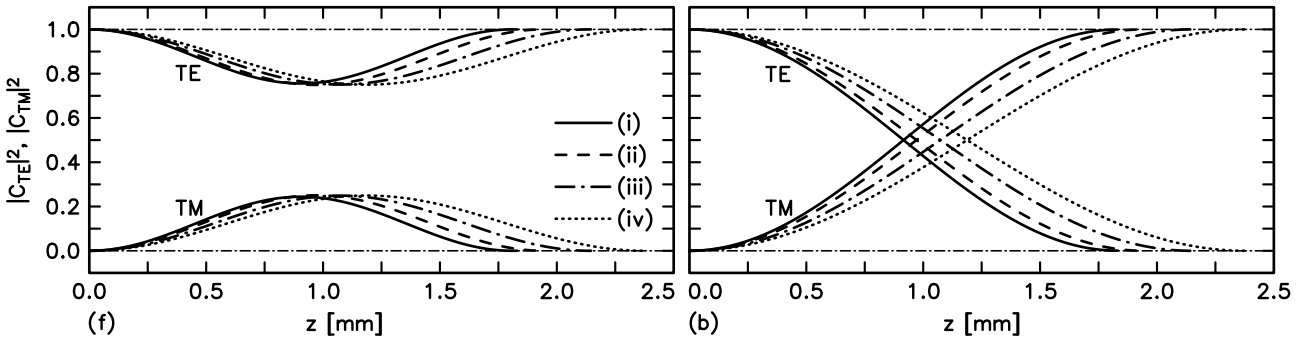


Figure 4: Relative mode powers  $|C_{\text{TE}}(z)|^2$ ,  $|C_{\text{TM}}(z)|^2$  for light propagation in the waveguides of Table 1 versus the propagation distance  $z$ , for forward (f) and backward propagation (b). The normalized TE mode is launched at  $z = 0$ .

Figure 4 illustrates the light propagation. While in forward direction the TE input is transformed to TM output, TE input leaves the device as TM polarized light in backward direction. Note that the waveguides work exactly analogously for TM input. In combination with polarization splitters, this enables the design of a polarization independent isolator, the simulation of which is the subject of the following section.

### 3 Polarization independent isolator/circulator

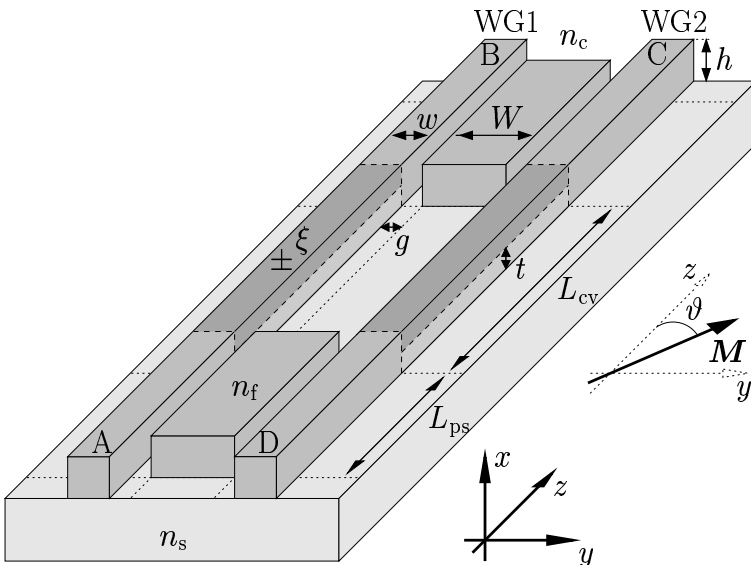


Figure 5: Geometry of the polarization independent circulator. The composite device consists of two polarization splitters, each of length  $L_{\text{ps}}$ , with two polarization converting double layer waveguides of length  $L_{\text{cv}}$  in-between. Letters A to D mark the four input and output ports.

Figure 5 sketches the concept. The polarization splitters are formed as three waveguide couplers with a multi-mode central strip of width  $W$ . Separated by gaps  $g$ , the central strip couples the two identical outer waveguides along a well defined length  $L_{ps}$ . Height  $h$  and width  $w$  of the outer waveguides are to be adapted to the polarization converters. Ref. [10] investigates similar three waveguide couplers in detail.

Table 2 collects a set of suitable parameters. The analysis of the composite device employs semivectorial WMM based coupled mode theory [10] for the polarization splitters, and a fully vectorial coupled mode formalism [5] for the magneto-optic polarization converters. The simulation proceeds stepwise along the five longitudinally homogeneous segments, with the output amplitudes of the four port modes from one waveguide segment used as input amplitudes for the subsequent one. For simplicity, we assume an isotropic material and positively and negatively rotating magneto-optic materials with the same refractive index. Then the port waveguide geometry  $h$ ,  $w$ , the length of the polarization converters  $L_{cv}$ , and the magneto-optic profile  $\xi$ ,  $t$ ,  $\vartheta$ , are dictated by the unidirectional phase matching condition (7), and by the requirement of backward phase matched waveguides. Table 2 shows parameters for waveguide (i) of Table 1. The planar waveguide ( $n_s$ ,  $n_f$ ,  $n_c$ ,  $h$ ) corresponding to the strips is still single mode, thus the polarization splitter design procedure of Ref. [10] can be applied, leading to the remaining dimensional parameters  $W$ ,  $g$ , and  $L_{ps}$ . We refer to Refs. [5, 10] for a detailed analysis of the fabrication tolerances of the involved components.

$h/\mu\text{m}$	$w/\mu\text{m}$	$t/\mu\text{m}$	$\vartheta/^\circ$	$g/\mu\text{m}$	$W/\mu\text{m}$	$L_{ps}/\mu\text{m}$	$L_{cv}/\mu\text{m}$	$n_s$	$n_f$	$n_c$	$\pm\xi$	$\lambda/\mu\text{m}$
0.634	0.798	0.181	63	0.103	3.616	492	1832	1.95	2.302	1.0	0.005	1.3

Table 2: Parameters enabling isolator performance of the device of Figure 5. The polarization converters and two polarization splitters add up to a total device length of 2.816 mm.

The simulation of the device serves best to explain its behaviour. Previously one should recall the function of the polarization splitters and of the unidirectional polarization converters. TM light injected in one of the polarization splitter ports leaves the splitter in the same waveguide straight ahead, while TE light changes the waveguide. This applies to both directions of light propagation. Waves propagating in the polarization converters in forward direction regain their input polarization at the output. In backward direction, TE input polarization is converted to TM output light, and vice versa. Combination of these functions leads to the light paths depicted in Figure 6. Charts (a) and (b) show a straight transmission from port A to B in forward direction for both input polarizations. In backward direction, illustrated in Figure 6 (c) and (d), port B is connected to D for TE and TM polarized light. Mirrored beating patterns appear for forward transmission from D to C and for the backward connection between C and A. This is the functionality of an isolator for the two straight light paths  $A \leftrightarrow B$  and  $D \leftrightarrow C$ .

An assessment of the device performance has to consider the polarization splitters first. The characteristic quantities are the relative power transmissions  $P_s$  for straight connections (WG1  $\rightarrow$  WG1, WG2  $\rightarrow$  WG2) and  $P_x$  for cross light paths (WG1  $\rightarrow$  WG2, WG2  $\rightarrow$  WG1) for TE and TM polarized light. Our analysis predicts extinction ratios of  $10 \log_{10}(P_s^{\text{TM}}/P_s^{\text{TE}}) = 26.3$  dB for the polarization discrimination in straight paths and  $10 \log_{10}(P_x^{\text{TE}}/P_x^{\text{TM}}) = 26.7$  dB for the cross connections. Losses due to mode mismatch at the waveguide junctions in the polarization splitters evaluate to  $-10 \log_{10}(P_x^{\text{TE}}) = 0.34$  dB for TE light and to  $-10 \log_{10}(P_s^{\text{TM}}) = 0.07$  dB for TM polarization.

In principle, properly adjusted parameters of the polarization converters enable ideal conversion. Then only the limited splitting ratios of the two polarization splitters bound the isolator performance. In backward direction, all power fractions pass a polarization splitter once in the TE and once in the TM polarization state. Hence the total relative backward power transmission from port B to A,  $P_{BA} = P_s^{\text{TE}} P_s^{\text{TM}} + P_x^{\text{TE}} P_x^{\text{TM}}$ , is independent from the input polarization. In forward direction, the power passes two polarization splitters in the input polarization state. The relative transmission is slightly polarization dependent. One obtains  $P_{AB} = \alpha((P_s^{\text{TE}})^2 + (P_x^{\text{TE}})^2) + (1 - \alpha)((P_s^{\text{TM}})^2 + (P_x^{\text{TM}})^2)$ , where  $\alpha$  is the ratio of TE over TM forward power input. If the device is employed as an isolator for the A-B connection, the simulation yields isolation levels  $10 \log_{10}(P_{AB}/P_{BA})$  of 23.3 dB and 23.7 dB and losses  $-10 \log_{10}(P_{AB})$  of 0.67 dB and 0.14 dB for TE and TM forward input polarization.

It depends on the definition of ‘ports’, whether the device can be regarded as a circulator. If the ports are defined in terms of modes, thus to be specified by a spatial outlet A to D and the mode polarization TE or TM,

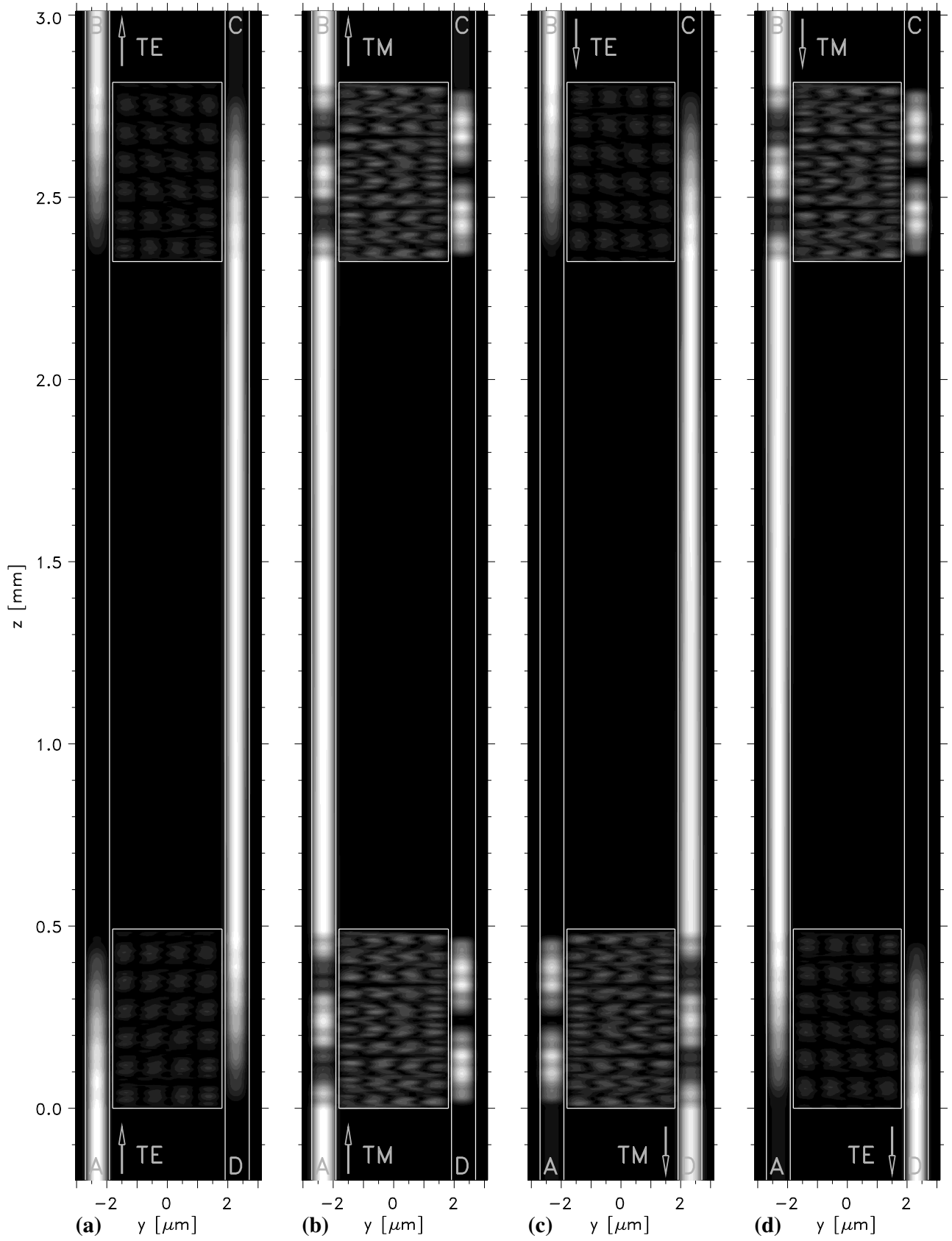


Figure 6: Light propagation through the device of Figure 5, with parameters as in Table 2. Grey scale levels indicate the squareroot of the local intensity (TE and TM part) in the  $y$ - $z$ -plane in the center of the guiding film at  $x = h/2$ . Arrows indicate the excited port, either TE or TM light is launched.

we obtain the two separate transmission cycles  $A_{TE} \rightarrow B_{TE}$ ,  $B_{TE} \rightarrow D_{TM}$ ,  $D_{TM} \rightarrow C_{TM}$ ,  $C_{TM} \rightarrow A_{TE}$ , and  $A_{TM} \rightarrow B_{TM}$ ,  $B_{TM} \rightarrow D_{TE}$ ,  $D_{TE} \rightarrow C_{TE}$ ,  $C_{TE} \rightarrow A_{TM}$ . There is no circulator functionality with respect to the four waveguides if only modes of equal polarization are admitted. If one considers input and output power only, the device performs as a polarization independent four port circulator with the transmission cycle  $A \rightarrow B$ ,  $B \rightarrow D$ ,  $D \rightarrow C$ ,  $C \rightarrow A$ .

In this paper we do not address the problem how to integrate the garnet waveguides and the non-magneto-optic polarization splitters on a common substrate. This is a difficulty with all concepts for real integrated nonreciprocal components unless the entire device is constructed from magneto-optic material. For the present circulator, etching the polarization splitters as well from the garnet double layer film may indeed be a solution: the vicinity of the central strip can be expected to disturb phase matching of the outer waveguides, preventing polarization conversion. Only TM polarized light is subject to a nonreciprocal phase shift, where the present magneto-optic structure should not cause a significant discrimination between forward and backward propagating light (a major effect would require an oppositely oriented magneto-optic profile in the outer waveguides [12]). However, without further simulations these statements are merely speculations.

## 4 Conclusions

A magneto-optic waveguide, which is magnetized at a certain angle with respect to the longitudinal direction, may perform as a unidirectional polarization converter. The term specifies a device that converts TE light to TM light (and vice versa) for one direction of propagation, while it maintains the polarization state for the opposite direction. This requires a balance of the gyrotropic effects of nonreciprocal phase shift and of polarization coupling. We proposed and simulated a setup with double layer waveguides, which are composed of magneto-optic films of opposite Faraday rotation. Two conditions of backward phase matching and forward phase detuning are to be met for ideal isolator performance. Both can be satisfied with proper adjustment of the geometric parameters and of the magneto-optic profile. The concept is a monolithic substitute for the conventional, usual hybrid configuration, where a nonreciprocal  $45^\circ$  polarization converter and a reciprocal  $45^\circ$  rotator are placed in line.

Combination of two magneto-optic unidirectional polarization converters and two polarization splitters leads to a design for a polarization independent isolator. If defined in terms of input/output power rather than in terms of mode amplitudes, this is a concept for a polarization independent integrated four port circulator device, to our knowledge the first ever proposed and simulated. For radiatively coupled waveguide based polarization splitters, our simulation predicts a total length of about three millimeters for optimistic, but still realistic material parameters.

## Acknowledgment

Financial support by Deutsche Forschungsgemeinschaft (Sonderforschungsbereich 225) is gratefully acknowledged.



## References

- [1] K. Ando, “Nonreciprocal devices for integrated optics,” *SPIE Proceedings*, vol. 1126, pp. 58–65, 1989.
- [2] N. Sugimoto, H. Terui, A. Tate, Y. Katoh, Y. Yamada, A. Sugita, A. Shibukawa, and Y. Inoue, “A Hybrid Integrated Waveguide Isolator on a Silica-Based Planar Lightwave Circuit,” *Journal of Lightwave Technology*, vol. 14, no. 11, pp. 2537–2546, 1996.
- [3] H. Iwamura, S. Hayashi, and H. Iwasaki, “A compact optical isolator using a  $Y_3Fe_5O_{12}$  crystal for near infra-red radiation,” *Optical and Quantum Electronics*, vol. 10, pp. 393–398, 1978.
- [4] T. Mizumoto and Y. Naito, “Waveguide-type optical isolator with in-plane magnetization structure,” in *Electro-Optic and Magneto-Optic Materials II*, H. Dammann, Ed., 1990, vol. 1274 of SPIE Proceedings, pp. 220–228.
- [5] M. Lohmeyer, N. Bahlmann, O. Zhuromskyy, H. Dötsch, and P. Hertel, “Phase-matched rectangular magneto-optic waveguides for applications in integrated optics isolators: numerical assessment,” *Optics Communications*, vol. 158, pp. 189–200, 1998.
- [6] M. Wallenhorst, M. Niemöller, H. Dötsch, P. Hertel, R. Gerhardt, and B. Gather, “Enhancement of the nonreciprocal magneto-optic effect of TM modes using iron garnet double layers with opposite Faraday rotation,” *Journal of Applied Physics*, vol. 77, no. 7, pp. 2902–2905, 1995.
- [7] T. Shintaku, “Integrated optical isolator based on nonreciprocal higher order mode conversion,” *Applied Physics Letters*, vol. 66, no. 21, pp. 2789–2791, 1995.
- [8] T. Shintaku, “Integrated optical isolator based on efficient nonreciprocal radiation mode conversion,” *Applied Physics Letters*, vol. 73, no. 14, pp. 1946–1948, 1998.
- [9] O. Zhuromskyy, M. Lohmeyer, N. Bahlmann, H. Dötsch, and P. Hertel, “Analysis of Polarization Independent Mach-Zehnder Type Integrated Optical Isolator,” *Journal of Lightwave Technology*, vol. 17, no. 7, pp. 1200–1205, 1999.
- [10] M. Lohmeyer, N. Bahlmann, O. Zhuromskyy, and P. Hertel, “Radiatively coupled waveguide polarization splitter simulated by wave-matching based coupled mode theory,” *Optical and Quantum Electronics*, 1999, Accepted for publication.
- [11] M. Lohmeyer, “Vectorial wave-matching mode analysis of integrated optical waveguides,” *Optical and Quantum Electronics*, vol. 30, pp. 385–396, 1998.
- [12] M. Lohmeyer, M. Shamonin, N. Bahlmann, P. Hertel, and H. Dötsch, “Radiatively coupled waveguide concept for an integrated magneto-optic circulator,” in *High-Density Magnetic Recording and Integrated Magneto-Optics: Materials and Devices*, K. Rubin, J. A. Bain, T. Nolan, D. Bogy, B. J. H. Stadler, M. Levy, J. P. Lorenzo, M. Mansuripur, Y. Okamura, and R. Wolfe, Eds., 1998, vol. 517 of MRS Symposium Proceedings Series, pp. 519–524.